Cumulene-like bridged indeno[1,2-b]fluorene π-conjugated polymers synthesized on metal surfaces

Cristina Martín-Fuentes, José I. Urgel,* Shayan Edalatmanesh, Eider Rodríguez-Sánchez, José Santos, Pingo Mutombo, Kalyan Biswas, Koen Lauwaet, José M. Gallego, Rodolfo Miranda, Pavel Jelínek,* Nazario Martín* and David Écija*

Cumulene-like bridged indeno[1,2-b]fluorene π-conjugated polymers synthesized on metal surfaces

Among the plethora of polycyclic structures that have emerged in recent years, indenofluorenes comprise a unique class of compounds due to their potential in organic electronic systems such as OLEDs, OFETs, and OPVCs. However, the synthesis of fully conjugated indenofluorenes without bulky groups on the apical carbons under standard chemistry conditions is not easily accessible. In this regard, on-surface synthesis has appeared as a newly developing field of research, which exploits the use of well-defined solid surfaces as confinement templates to initiate and develop chemical reactions. Here, we demonstrate the successful fabrication of indeno[1,2-b]fluorene π-conjugated polymers linked via cumulene-like connections on well-defined metallic surfaces UNDER ULTRA-HIGH VACUUM CONDITIONS. The structure and electronic properties of the formed polymers have been precisely characterized by scanning tunneling microscopy, noncontact atomic force microscopy and scanning tunneling spectroscopy, complemented by computational investigations.

The engineering of π-conjugated polymers is a highly active area of research given their relevance in organic light emitting diodes, organic field effect transistors and organic photovoltaic cells.[1–5] A special effort in the area has been devoted to bridged phenylene-based polymers,[6] with fluorene, indenofluorene and higher ladder type phenylenes as repeat units, due to their great potential in electronic applications. Specifically, the family of indenofluorenes (sequence of fully conjugated five fused rings with 6, 5, 6, 5, and 6 carbon atoms) and their derivatives, have been identified as promising candidates for stable light emission and more recently as semiconducting material in devices.[7,8] The presence of five-membered rings in their structure enables the existence of five structural isomers which may exhibit unique optical properties arising from the unsymmetrical distribution between their frontier orbitals. Since the first reported synthesis of an indenofluorene scaffold in the late nineteenth century, an extensive effort has been devoted to their solution synthesis.[9] However, the inherent reactivity of this family of polycyclic aromatic hydrocarbons has limited their practical applications[10] as well as their solution synthesis without the presence of protecting groups located at the most reactive positions.[11–15]

On-surface synthesis allows us to overcome some of these difficulties, frequently encountered in solution chemistry of highly reactive compounds. It is also a powerful strategy to design and study atomistically precise nanomaterials on single-crystal surfaces under ultrahigh-vacuum (UHV) conditions. These experimental conditions allow for the visualization of the resulting products at the ultimate spatial scale.[16] For instance, the on-surface chemistry paradigm has been employed to engineer π-conjugated polymers of distinct complexity including one-dimensional and ladder-type polymers that are difficult or not possible to achieve in solution. However, on surfaces there is still limited knowledge about synthetic protocols and properties of indenofluorenes[17,18] and polymers based on them.[19–21] Herein, it is of crucial importance to incorporate more complex bridges in order to specifically tailor the dominant resonance form in nonbenzenoid carbon materials and specifically on polyindenofluorenes, thus taming the resulting physico-chemical properties.

In this communication, we introduce an extensive STM, scanning tunneling spectroscopy (STS), non-contact atomic force microscopy (nc-AFM), temperature programmed desorption experiments (TPD) and density functional theory (DFT) investigation of the on-surface formation of cumulene-linked indenofluorene polymers (**3**) adsorbed on several noble metal surfaces under ultrahigh vacuum (UHV) conditions. To this end, we have synthesized in solution the precursor **1** which consists of an indeno[1,2-b]fluorene backbone as the core motif, equipped

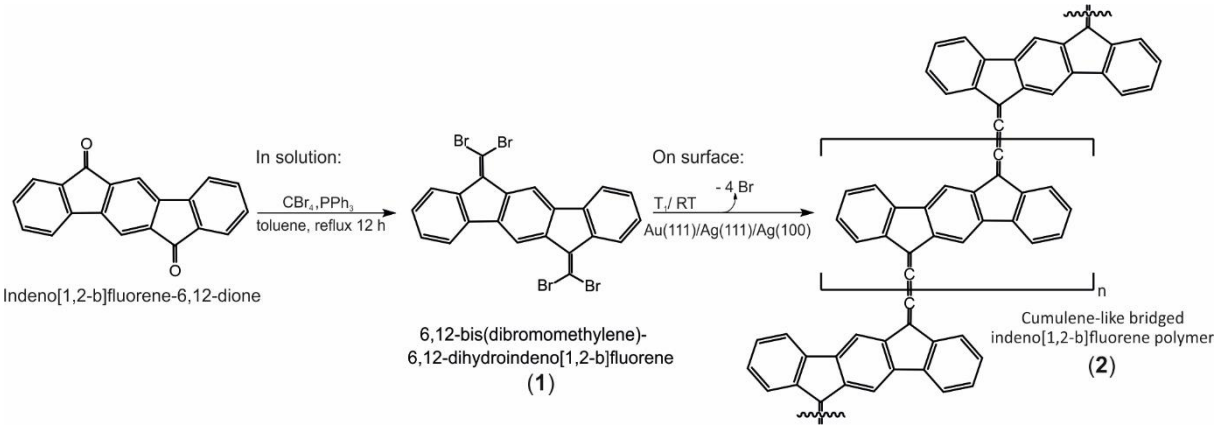

Scheme 1. Synthetic route toward the formation of cumulene-linked indeno[1,2-b]fluorene polymers.

with two additional dibromomethylenes attached to the pentagonal moiety (see Supporting Information for synthetic details). Subsequently, **1** is sublimed intact on the surface and transformed into **2** by thermal activation (Scheme 1), following a synthetic pathway based on the loss of bromine atoms and homocouple of the carbene moities.[22–27] Our work provides prospects toward the synthesis and characterization of nonbenzenoid polycyclic aromatic hydrocarbons containing five-membered rings, with possible applications in fields such as molecular spintronics, nonlinear optics, organic light emission, lasers and organic photovoltaic devices.

Submonolayer deposition of **1** onto an atomically clean Au(111) surface held at room temperature (RT) and subsequent annealing to 200°C (T_1 in the Scheme), reveals the appearance of 1D polymers composed of rectangle-shaped units, as observed in the large-scale STM image (Figure 1a). The formation of such polymers is attributed to the debromination of **1,** followed by C-C coupling, after the annealing process, with the detached bromine atoms observed as rounded protrusions bound to the gold substrate in the vicinity of the polymers. In addition, Figure 1b,c show the formation of similar 1D polymers after RT deposition of **1** on Ag(111) and Ag(100), where the activation temperature needed for dehalogenation is lower than on Au(111).[28] Figure 1d displays a zoom-in STM image acquired on Au(111), which together with nc-AFM measurements using a CO-functionalized tip[29] allows us to evaluate the intramolecular features of **2**. Herein, Figure 1e depicts the resulting constant-height frequency-shift image, where four indeno[1,2-b]fluorene units linked to each other by sharp lines through their apical positions (C6 and C12) of the five-membered rings are clearly discerned (see Figure S1 for high-resolution STM and nc-AFM images of **2** on Ag(111)). Such features, observed in the intermolecular connections of **2**, are attributed to cumulene-like bonds, with a C-C distance between cumulene bonds of 4.0 $\pm$ 0.2 Å.[25] TPD experiments reveal that further annealing of the sample till 450°C induces the bromine desorption (with a maximum desorption rate at 360°C), which predominantly occurs via hydrogenation of the bromine atoms (HBr) as depicted in Figure 1f, being in agreement with previous studies.[30,31] We attribute this hydrogenation to the existence of residual hydrogen gas in the vacuum chamber.

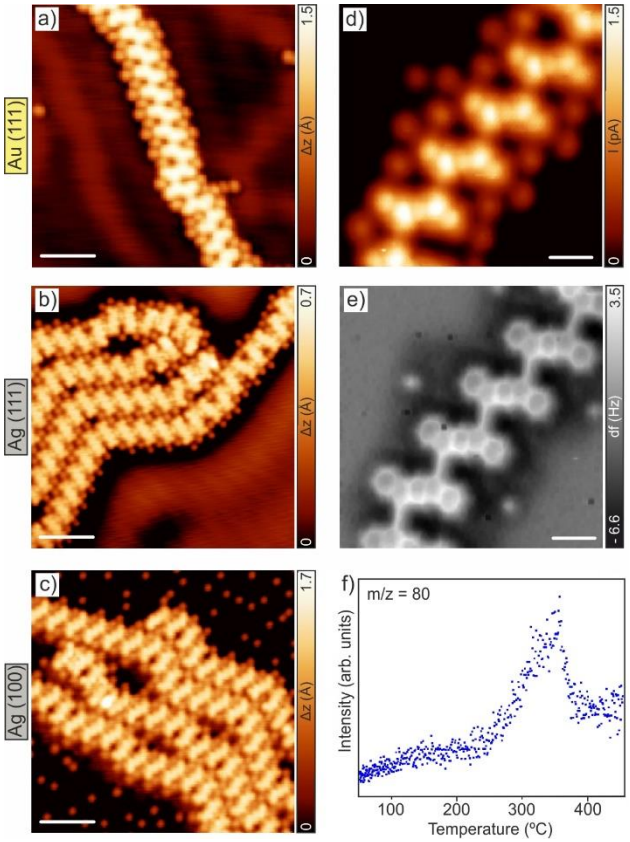

Fig. 1 On-surface synthesis and structural characterization of cumulene-like bridged indeno[1,2-b]fluorene polymers on metal surfaces. a-c) High-resolution STM images of the sample after deposition at RT of a submonolayer coverage of 1 on Ag(111) and Ag(100) and, in the case of Au(111), after subsequent annealing at 200°C. Scanning parameters: V_b = 50 mV, I_t = 50 pA, scale bar = 2 nm. (d) Zoom-in high-resolution constant-height STM image of a polymer chain comprising four indeno[1,2-b]fluorene units. Scanning parameters: V_b = 5 mV, I_t = 100 pA, scale bar = 0.5 nm. (e) Constant-height frequency-shift nc-AFM image of (d) acquired with a CO-functionalized tip. Open feedback parameters: V_b = 5 mV. Scale bar = 0.5 nm. (f) TPD graph which depicts the desorption of HBr molecules from the Au(111) surface with a maximum desorption rate at 360°C (heating rate 2°C /s).

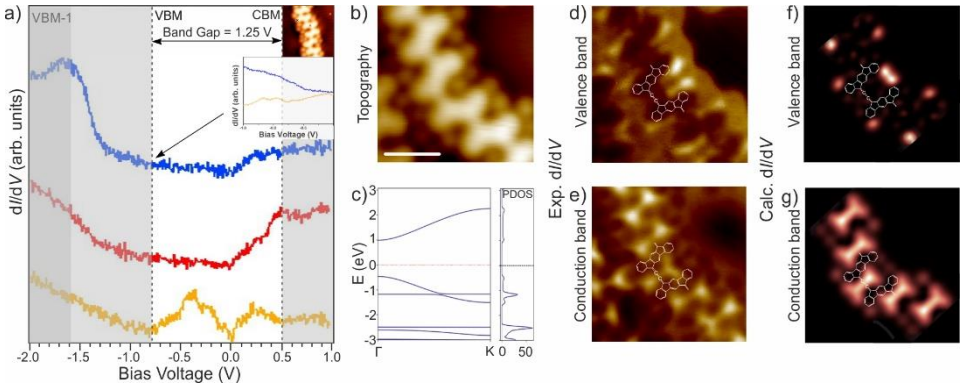

Fig. 2 Characterization of the electronic structure of 2 on Au(111). a) d*I*/d*V* spectra acquired on 2 (blue and red curves) and on the gold surface (orange curve) at the positions marked with blue, red and orange crosses at the STM image placed at the top of (a), V_b = 50 mV, I_t = 10 pA. Due to the strong contribution of the VB -1 it is difficult to elucidate the VBM, whose contribution is depicted in a separate d*I*/d*V* spectra below the STM image. (b) High-resolution STM images of the polymeric segment where d*I*/d*V* maps were acquired. V_b = 100 mV, I_t = 100 pA, scale bar = 1 nm. c) Calculated band structure and PDOS of free-standing infinite polymer 2. d-g) Constant-current differential conductance (dI/dV) maps (d,e) and corresponding DFT calculated d*I*/d*V* maps (f,g) at the energetic positions shown in (a). Tunneling parameters for the d*I*/d*V* maps: VB (V_b = -0.75 V, I_t = 200 pA); CB (V_b = 0.50 V, I_t = 300 pA).

Furthermore, it is worth mentioning that the two possible ways that **1** can adsorb on a surface due to its 2D confinement may lead to an expression of chirality. A statistical analysis of the polymer (out of more than 1400 molecules) indicates that both E/Z isomers forming the polymers are observed in similar amounts (≈50%) regardless of the employed surface. However, in the case of **2** formed on Ag(111) and Ag(100), we found that a non-negligible amount (≈60% and ≈70%, respectively) of indeno[1,2-b]fluorene units observed in the polymers prefer to be connected to the same enantiomer (representative large scale STM images are reported in Figure S2). This fact is tentatively attributed to minute differences in adsorption energy. As a result, larger regioregular segments, whereby the monomers exhibit identical energy fingerprint on the surface, are favoured as compared to regiorandom sections in which the monomers display two different registries with the substrate, thus introducing an energetic penalty.

Finally, in order to elucidate the electronic properties of **2** studied on Au(111), we have conducted STS measurements. Figure 2a shows the differential conductance (d*I*/d*V*) spectrum recorded on distinct positions of a segment of **2** displaying features in the density of states. On one hand, it is observed a resonance peak at 0.50 V, which is assigned to the conduction band maximum (CBM, see below).On the other hand, the occupied density of states is dominated by a strong resonance peak at -1.58 V, which is interpreted as the valence band minimum (VBM)-1 (see Fig. S3). The valence band (VB) is not clearly visible and it simply displays an increase of the density of states in point STS as seen in the inset of Figure 2. In order to visualize the spatial distribution of the bands and to set the valence band minimum (VBM), we took constant-current maps of the d*I*/d*V* signal at selected biases and compared them to DFT theoretical calculations.[32,33] We set the VBM at -0.75 eV, an energetic position where the d*I*/d*V* map already displays its distinct shape. Importantly, there is a good agreement between experimental and calculated d*I*/d*V* maps, which confirms our interpretation of the electronic band structure. Therefore, the measured band gap of this polymer is 1.25 eV on Au(111), which is 0.2 eV lower than the value obtained from the calculated band structure of the free-standing polymer (1.42 eV). Such a small difference in band gap between theory and experiment is attributed to the increased screening effect introduced by the underlying metallic substrate (Figure 2c) and to the experimental uncertainty in determining the VBM.[34] Interestingly, the biradical character among the five existing indenofluorene isomers might be drastically different ranging from closed-shell to open-shell.[35,36] In fact, aryl-aryl bridged polymers formed on the Au(111) surface and based on indeno[1,2-b]fluorenes are expected to be closed-shell featuring a bandgap of 1.25 eV, whereas those based on indeno[2,1-b]fluorene were reported to be open-shell, exhibiting a narrow band-gap of 0.4 eV. In our case, **2** follows the Clar´s sextet rule, thus maximizing the expression of three Clar sextets, which gives rise to a resonance form in which the bridge is cumulene-like and the monomer is aromatic, without open-shell character. The same mechanism applies on Ag(111), where again a cumulene-bridged resonance form is detected (see Figure S1). Notably, such a pro-aromatic mechanism is worth to be pointed out as a way to control the expression of open-shell character in carbon nanomaterials[37] while designed on surfaces.

In summary, we have introduced protocols for the fabrication of cumulene-linked indeno[1,2-b]fluorene polymers synthesized on noble metal surfaces. The formed polymer **2** has been unambiguously characterized by STM and nc-AFM, which unveils the cumulene-like nature of the polymer connections. Additionally, STS studies together with theoretical calculations reveal that **2** exhibits an electronic gap of 1.25 eV and a closed-shell electron configuration adsorbed on Au(111). We expect that our investigation is of common relevance for the synthesis and characterization of conjugated polymers incorporating five- membered rings, paving the way to further investigation of indenofluorene polymers and opening novel avenues in the field of on-surface synthesis with prospects for applications in molecular electronics.

We acknowledge the Comunidad de Madrid [project QUIMTRONIC-CM(Y2018/NMT-4783)], the ECFP7-PEOPLE-2011 COFUND AMAROUT II, and Ministerio de Ciencia e Innovación (PID2019-108532GB-I00). IMDEA Nanociencia thanks support from the ''Severo Ochoa'' Programme for Centers of Excellence in R&D (MINECO, Grant SEV-2016-0686). P.J. acknowledges support from Praemium Academie of the Academy of Science of the Czech Republic, GACR20-13692X. Computational resources were provided by the CESNETLM2015042 and the CERIT Scientific Cloud LM2015085. J.I.U. thanks the funding from the European Union's Horizon 2020 research and innovation programme under the Marie Skłodowska-Curie grant agreement No. [886314].

Notes and references

1 A. Facchetti, *Chem. Mater.*, 2011, **23**, 733–758.
2 O. Ostroverkhova, *Chem. Rev.*, 2016, **116**, 13279–13412.
3 R. Lakshmanan and S. C. G. Kiruba Daniel, in *Handbook of Nanomaterials for Industrial Applications*, ed. C. Mustansar Hussain, Elsevier, 2018, pp. 312–323.
4 A. J. Heeger, *Angew. Chem. Int. Ed.*, 2001, **40**, 2591–2611.
5 X. Guo, M. Baumgarten and K. Müllen, *Prog. Polym. Sci.*, 2013, **38**, 1832–1908.
6 A. C. Grimsdale and K. Müllen, in *Polyfluorenes*, eds. U. Scherf and D. Neher, Springer, Berlin, Heidelberg, 2008, pp. 1–48.
7 H. Usta, A. Facchetti and T. J. Marks, *J. Am. Chem. Soc.*, 2008, **130**, 8580–8581.
8 H. Usta, C. Risko, Z. Wang, H. Huang, M. K. Deliomeroglu, A. Zhukhovitskiy, A. Facchetti and T. J. Marks, *J. Am. Chem. Soc.*, 2009, **131**, 5586–5608.
9 A. G. Fix, D. T. Chase and M. M. Haley, in *Polyarenes I*, eds. J. S. Siegel and Y.-T. Wu, Springer Berlin Heidelberg, 2012, pp. 159–195.
10 A. M. Zeidell, L. Jennings, C. K. Frederickson, Q. Ai, J. J. Dressler, L. N. Zakharov, C. Risko, M. M. Haley and O. D. Jurchescu, *Chem. Mater.*, 2019, **31**, 6962–6970.
11 A. Shimizu and Y. Tobe, *Angew. Chem.*, 2011, **123**, 7038–7042.
12 D. T. Chase, B. D. Rose, S. P. McClintock, L. N. Zakharov and M. M. Haley, *Angew. Chem. Int. Ed.*, 2011, **50**, 1127–1130.
13 A. G. Fix, P. E. Deal, C. L. Vonnegut, B. D. Rose, L. N. Zakharov and M. M. Haley, *Org. Lett.*, 2013, **15**, 1362–1365.
14 G. E. Rudebusch, J. L. Zafra, K. Jorner, K. Fukuda, J. L. Marshall, I. Arrechea-Marcos, G. L. Espejo, R. Ponce Ortiz, C. J. Gómez-García, L. N. Zakharov, M. Nakano, H. Ottosson, J. Casado and M. M. Haley, *Nat. Chem.*, 2016, **8**, 753–759.
15 C. K. Frederickson, B. D. Rose and M. M. Haley, *Acc. Chem. Res.*, 2017, **50**, 977–987.
16 Q. Shen, H.-Y. Gao and H. Fuchs, *Nano Today*, 2017, **13**, 77–96.
17 Z. Majzik, N. Pavliček, M. Vilas-Varela, D. Pérez, N. Moll, E. Guitián, G. Meyer, D. Peña and L. Gross, *Nat. Commun.*, 2018, **9**, 1198.
18 R. Zuzak, O. Stoica, R. Blieck, A. M. Echavarren and S. Godlewski, *ACS Nano*, 2021, **15**, 1548–1554.
19 M. Di Giovannantonio, J. I. Urgel, U. Beser, A. V. Yakutovich, J. Wilhelm, C. A. Pignedoli, P. Ruffieux, A. Narita, K. Müllen and R. Fasel, *J. Am. Chem. Soc.*, 2018, **140**, 3532–3536.
20 M. Di Giovannantonio, K. Eimre, A. V. Yakutovich, Q. Chen, S. Mishra, J. I. Urgel, C. A. Pignedoli, P. Ruffieux, K. Müllen, A. Narita and R. Fasel, *J. Am. Chem. Soc.*, 2019, **141**, 12346–12354.
21 M. Di Giovannantonio, Q. Chen, J. I. Urgel, P. Ruffieux, C. A. Pignedoli, K. Müllen, A. Narita and R. Fasel, *J. Am. Chem. Soc.*, 2020, **142**, 12925–12929.
22 Q. Sun, B. V. Tran, L. Cai, H. Ma, X. Yu, C. Yuan, M. Stöhr and W. Xu, *Angew. Chem. Int. Ed.*, 2017, **56**, 12165–12169.
23 A. Sánchez-Grande, B. de la Torre, J. Santos, B. Cirera, K. Lauwaet, T. Chutora, S. Edalatmanesh, P. Mutombo, J. Rosen, R. Zbořil, R. Miranda, J. Björk, P. Jelínek, N. Martín and D. Écija, *Angew. Chem. Int. Ed.*, 2019, **58**, 6559–6563.
24 B. Cirera, A. Sánchez-Grande, B. de la Torre, J. Santos, S. Edalatmanesh, E. Rodríguez-Sánchez, K. Lauwaet, B. Mallada, R. Zbořil, R. Miranda, O. Gröning, P. Jelínek, N. Martín and D. Ecija, *Nat. Nanotechnol.*, 2020, **15**, 437–443.
25 J. I. Urgel, M. D. Giovannantonio, K. Eimre, T. G. Lohr, J. Liu, S. Mishra, Q. Sun, A. Kinikar, R. Widmer, S. Stolz, M. Bommert, R. Berger, P. Ruffieux, C. A. Pignedoli, K. Müllen, X. Feng and R. Fasel, *Angew. Chem.*, 2020, **132**, 13383–13389.
26 A. Sánchez-Grande, J. I. Urgel, A. Cahlík, J. Santos, S. Edalatmanesh, E. Rodríguez-Sánchez, K. Lauwaet, P. Mutombo, D. Nachtigallová, R. Nieman, H. Lischka, B. de la Torre, R. Miranda, O. Gröning, N. Martín, P. Jelínek and D. Écija, *Angew. Chem. Int. Ed.*, 2020, **59**, 17594–17599.
27 K. Biswas, J. I. Urgel, A. Sánchez-Grande, S. Edalatmanesh, J. Santos, B. Cirera, P. Mutombo, K. Lauwaet, R. Miranda, P. Jelínek, N. Martín and D. Écija, *Chem. Commun.*, 2020, **56**, 15309–15312.
28 M. Fritton, D. A. Duncan, P. S. Deimel, A. Rastgoo-Lahrood, F. Allegretti, J. V. Barth, W. M. Heckl, J. Björk and M. Lackinger, *J Am Chem Soc*, 2019, **141**, 4824–4832.
29 L. Gross, F. Mohn, N. Moll, P. Liljeroth and G. Meyer, *Science*, 2009, **325**, 1110–1114.
30 C. Bronner, J. Björk and P. Tegeder, *J. Phys. Chem. C*, 2015, **119**, 486–493.
31 M. Di Giovannantonio, O. Deniz, J. I. Urgel, R. Widmer, T. Dienel, S. Stolz, C. Sánchez-Sánchez, M. Muntwiler, T. Dumslaff, R. Berger, A. Narita, X. Feng, K. Müllen, P. Ruffieux and R. Fasel, *ACS Nano*, 2018, **12**, 74–81.

32 S. Hoshino, *Phys. Rev. B*, 2014, **90**, 115154.
33 O. Krejčí, P. Hapala, M. Ondráček and P. Jelínek, *Phys. Rev. B*, 2017, **95**, 045407.
34 J. B. Neaton, M. S. Hybertsen and S. G. Louie, *Phys. Rev. Lett.*, 2006, **97**, 216405.
35 K. Fukuda, T. Nagami, J. Fujiyoshi and M. Nakano, *J. Phys. Chem. A*, 2015, **119**, 10620–10627.
36 A. G. Fix, D. T. Chase and M. M. Haley, in *Polyarenes I*, eds. J. S. Siegel and Y.-T. Wu, Springer, Berlin, Heidelberg, 2014, pp. 159–195.
37 J. Casado, in *Physical Organic Chemistry of Quinodimethanes*, eds. Y. Tobe and T. Kubo, Springer International Publishing, Cham, 2018, pp. 209–248.